Investigation of the degradation and *in-situ* amorphization of the enantiomeric drug escitalopram oxalate during Fused Deposition Modeling (FDM) 3D printing

Lena Hoffmann [a], Jörg Breitkreutz [a], Julian Quodbach [b,*]

[a] *Institute of Pharmaceutics and Biopharmaceutics, Heinrich Heine University, Universitätsstraße 1, 40225 Düsseldorf, Germany*
[b] *Department of Pharmaceutics, Utrecht University, Universiteitsweg 99, 3584 CG Utrecht, the Netherlands*

ARTICLE INFO

ABSTRACT

Hot-melt extrusion (HME) and subsequent FDM 3D printing offer great potential opportunities in the formulation development and production of customized oral dosage forms with poorly soluble drugs. However, thermal stress within these processes can be challenging for thermo-sensitive drugs. In this work, three different formulations were prepared to investigate the degradation and the solid state of the thermo-sensitive and poorly soluble drug escitalopram oxalate (ESC-OX) during the two heat-intensive processes HME and FDM 3D printing. For this purpose, hydroxypropyl methyl cellulose (HPMC) and basic butylated methacrylate copolymer (bPMMA) were chosen as polymers. DSC and XRD measurements revealed that ESC-OX is amorphous in the HPMC based formulations in both, extrudates and 3D printed tablets. In contrast, *in-situ* amorphization of the drug from crystalline state in bPMMA filaments was observed during FDM 3D printing. With regard to the content, it was found that degradation of ESC-OX in extrudates with bPMMA could be avoided and in 3D printed tablets almost fully reduced. Furthermore, a possible conversion into the R-enantiomer in the formulation with bPMMA could be excluded using a chiral column. Compared to the commercial product Cipralex®, drug release from extrudates and tablets with bPMMA was slower but still qualified as immediate drug release.

1. Introduction

Fused deposition modeling (FDM) 3D printing is an additive manufacturing technique, which is widely explored in pharmaceutics for the production of personalized dosage forms (Khalid and Billa, 2022). It offers the opportunity to manufacture dosage forms with an individual dose and desired release profile on-demand in short time. Therefore, the dose can be adapted to the special needs of the patients (Awad et al., 2018; Konta et al., 2017; Fernandez-Garcia et al., 2020; Windolf, et al. 2022) as well as the needs of pediatric and geriatric patients (Scoutaris et al., 2018; Krause et al., 2021; Hoffmann et al., 2022a). This becomes increasingly important in personalized medicine (Goyanes et al., 2017; Varghese et al., 2022) and can also be beneficial in pandemic situations when shortages are present (Khalid and Billa, 2022).

To meet the growing interest in FDM 3D printed dosage forms, hot-melt extrusion can be applied for the production of filaments, the feedstock material for the subsequent 3D printing process (El Aita et al., 2018, Hoffmann et al., 2022b). HME, as an upstream process, can be considered as preferred method for the preparation of amorphous solid dispersions (ASDs) which can improve the solubility of poorly soluble drugs (Pawar et al., 2016; Tan et al., 2020). Besides the solubility enhancement of BCS class II and IV drugs, HME can improve bioavailability and dissolution rate (Douroumis, 2012; Kanaujia et al., 2015). This becomes a major concern in the pharmaceutical industry, because 40 % of approved medicines and up to 90 % of drugs in the discovery pipeline are poorly water soluble (Hiew et al., 2022; Kalepu and Nekkanti, 2015).

The production of amorphous solid dispersions should overcome this problem by converting the drug from the crystalline state to the amorphous state (Grohganz et al., 2013). However, the amorphous drug must be stabilized in a (polymer) matrix, prolonging the stability of the amorphous state and preventing recrystallization (Holm et al., 2022). Therefore, the combination of hot-melt extrusion followed by FDM 3D printing should enable the possibility to improve on the one hand, the solubility issues and, on the other hand, the production of customized 3D printed oral dosage forms with poorly soluble drugs. This is

---

* Corresponding author.
  E-mail address: j.h.j.quodbach@uu.nl (J. Quodbach).

beneficial because oral dosage forms are still the preferred choice due to their ease of administration (Alhnan et al., 2016; Wang et al., 2022). Nevertheless, the combination of the two processes, hot-melt extrusion and FDM 3D printing, also have drawbacks. Thermo-sensitive drugs are subjected to high temperatures twice (Khalid and Billa, 2022).

Hence, the processing of thermo-sensitive drugs can be challenging (Abdella, et al. 2021; Kempin, et al. 2018). The first investigations were conducted by Goyanes et al. (2015), who explored the thermal degradation of 5-aminosalicylic acid (5-ASA) and 4-aminosalicylic acid (4-ASA) from previously made filaments during FDM 3D printing. It was shown that the degradation of the active ingredients during FDM 3D printing at a temperature of 210°C was drug dependent. 4-aminosalicyclic acid, which initially melts and then decomposes at a temperature between 130 to 145°C, degraded to 50 %, while the drug 5-aminosalicylic acid was stable with a melting temperature of 278 to 279°C. Kollamaram et al. (2018) prepared filaments with the model drug ramipril, which has a low melting temperature of 109°C, and the two immediate release polymers Kollidon VA 64 and Kollidon 12 PF via hot-melt extrusion at a temperature of 70°C. They used them as feedstock material for the production of 3D printed tablets via FDM 3D printing at a temperature of 90°C. Kempin et al. (2018) investigated the drug pantoprazole sodium, which is not only thermo-labile but also acid-labile during both heat-intensive processes HME and FDM. A thermal degradation of the active ingredient was observed during dual extrusion printing with a cellulose acetate phthalate coating and a tablet core of polyethylene glycol 6.000 at a printing temperature of 141°C. After development of different tablets designs, the design of a tablet coating with a gastro-resistant cellulose acetate phthalate bottom part and an upper, nearly insoluble polycaprolactone part resulted in a printing temperature of 58°C and no signs of degradation. Furthermore, Manini et al. (2022) produced implants with the heat-sensitive active ingredient paliperidone palmitate below a temperature of 180°C to avoid thermal degradation, due to the degradation temperature at approximately 180°C and investigate the stability of the solid state and the release behavior of the implants over three months. Until now, the possibility of thermally induced racemization has not been investigated.

For the present study, we selected the chiral drug ESC-OX as model drug for the investigations of both the thermal instability and also the solid state during hot-melt extrusion and FDM 3D printing. ESC-OX is a selective serotonin (5-HT) reuptake inhibitor (SSRI) which is used for the treatment of major depressive disorder (MDD) and several anxiety disorders (Jagtap and Bhaskar, 2013). According to the WHO, mental disorders, with anxiety and depressive disorders as most common, affected approximately 970 million people in 2019 (Institute of Health Metrics and Evaluation. Global Health Data Exchange (GHDx), 2022). From these, 301 million people suffered from anxiety disorder and 280 million people suffered from depression (Institute of Health Metrics and Evaluation. Global Health Data Exchange (GHDx), 2022). Due to the COVID-19 pandemic, the Global Burden of Disease (GBD) 2020 estimated that the number of people suffering from these diseases increased significantly by 25.6 % and 27.6 % respectively within one year (Santomauro et al., 2021). SSRIs are considered as first-line treatment in antidepressant medication (Waugh and Goa, 2003) and are characterized by good tolerability due to the high selectivity and low interaction potential compared to other antidepressants (Kirino, 2012; O'Donnell and Shelton, 2015). Escitalopram (ESC) is the S-stereoisomer of racemic
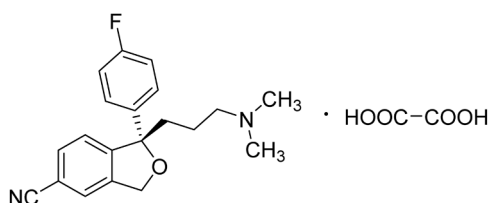
(R,S) citalopram (Fig. 1) (Pinto et al., 2018) and has been shown to have greater efficacy than the racemate citalopram while being equally well tolerated (Cipriani et al., 2009; Gartlehner et al., 2011; Cipriani et al., 2009).

ESC-OX is listed on the WHO Model List of Essential Medicines (WHO, 2021) and is marketed by Lundbeck GmbH under the trade names Cipralex® and Lexapro® (Akay et al., 2021). It is administered orally, with the dose equal to the free base (Akay et al., 2021). Although the oxalate salt is administered, the drug belongs to the BCS class II drugs with low solubility and high permeability (Akay et al., 2021). In addition to the poor solubility, ESC-OX also shows a pronounced pH instability in basic solution (Rao et al., 2008; Dhaneshwar et al., 2008).

Thus, the main aim of this work was to investigate the thermal degradation of the thermo-sensitive and base-labile antidepressant ESC-OX and its degradation products during hot-melt extrusion and FDM 3D printing depending on a neutral and basic polymer matrix used. This also includes the investigations of a possible conversion of the enantiomer S-Citalopram into R-Citalopram during these two heat-intensive processes. Formulation development was carried out to prevent degradation of ESC-OX leading to the optimized formulation F3. Besides the chemical stability, the physical state of ESC-OX embedded in the different polymer matrices during HME and FDM 3D printing was examined. Lastly, the optimized formulation with the polymer bPMMA was compared with the commercially available Cipralex® 10 mg filmcoated tablets regarding the physical state, the purity as well as dissolution.

2. Materials and methods

2.1. Materials

ESC-OX was purchased from F. & A. Pharma-Handels-GmbH (Marl, Germany) ex Micro Labs Limited (Bangalore, India). Hypromellose (HPMC, Affinisol™ HPMC HME 15 LV) and polyethylene oxid Mw 100.000 (PEO, Polyox™ WSR N10) were kindly provided by DuPont Nutrition & Biosciences (Neu-Isenburg, Germany). Basic butylated methacrylate copolymer (bPMMA, Eudragit® E PO) and fumed silica (Aerosil® 200 V/V Pharma) were kindly provided by Evonik (Essen, Germany). Polyethylene glycol (PEG) 6.000 (Polyglykol® 6000 P) was kindly provided by Clariant (Frankfurt, Germany). ESC-OX United States Pharmacopoeia (USP) reference standard, R-Citalopram oxalate USP reference standard, Citalopram Related Compound A USP reference standard (CIT-A), Citalopram Related Compound B USP reference standard (CIT-B) and Citalopram Related Compound C USP reference standard (CIT-C) were purchased by Eurofins PHAST GmbH (Homburg, Germany). Citalopram hydrobromide CRS was purchased at the European Directorate for the Quality of Medicine & Healthcare (Strasbourg, France).

2.2. Preparation of drug loaded extrudates

Hot-melt extrusion was carried out for the production of extrudates. Extrudates were prepared with three different formulations (Table 1).

To ensure a homogenous powder mixture of each formulation, ESC-OX and the polymers were separately sieved (355 μm) and mixed for 15 min in a turbula mixer (T2F, Willy A. Bachofen, Switzerland). The higher amount of SiO_2 in F3 compared to formulations F1 and F2 was used to improve the flowability of this powder mixture. The formulations were fed with a flat-bottom powder feeder (ZD 5 FB, Three-Tec, Seon, Switzerland) at a feed rate of 100 g/h into a co-rotating twin screw extruder (ZSE12 HP-PH, Leistritz, Nürnberg, Germany) with a screw diameter of 12 mm. Screws with two kneading zones and a die with a diameter of 2 mm were used. The extrusion temperature profiles are detailed in Table 2. The screw speed was set to 25 rpm in all cases.

Following the extrusion, the extruded strand was cooled and transported with a conveyor belt (model 846102.001, Brabender, Germany).

Fig. 1. Structural formula of ESC-OX.

Table 1

Formulation composition for the production of HME extrudates (w/w).

Formulation	API (%)		Matrix (%)				Plasticizer (%)		Glidant (%)	
F1	ESC-OX	12.78	HPMC	81.72	bPMMA	-	PEG 6.000	5	SiO$_2$	0.5
F2	ESC-OX	12.78	HPMC	71.72	bPMMA	10	PEG 6.000	5	SiO$_2$	0.5
F3	ESC-OX	12.78	-	-	bPMMA	42.61	PEO	42.61	SiO$_2$	2.0

Table 2

Temperature profiles across the different zones of the extruder barrel (°C).

Formulation	Zone 1	2	3	4	5	6	7	8	Die
F1 / F2	20	20	150	150	150	150	150	150	150
F3	20	20	80	80	80	80	80	80	80

The desired extrudate diameter of 1.75 mm was achieved using a belt hauled-off unit of a winder (Brabender, Duisburg, Germany).

2.3. 3D printing of ESC-OX tablets

The extrudates were printed with a 0.4 mm nozzle into tablets using a FDM 3D printer (i3 Mk3, Prusa Research; Czech Republic). The tablet geometry was designed using Autodesk Fusion 360 (Mill Valley, USA) and then sliced using the PrusaSlicer (PRUSA Research; Hradec Králové, Czech Republic). For formulation F1 and F2, the extrudates were printed at 180°C nozzle temperature and 65°C print bed temperature with a printing speed of 30 mm/s. For formulation F3, the extrudates were printed at 180°C nozzle temperature and 35°C print bed temperature with a printing speed of 30 mm/s. A cylindrical tablet geometry (diameter: 6.8 mm and height: 2.4 mm) was selected to obtain a 100 mg tablet with a dose of 10 mg and a drug loading of 10 % ESC. All tablets were printed with a layer height of 0.2 mm and 100 % infill.

2.4. Microscopy

Images of the tablets were taken using a Keyence digital microscope VHX-6000 (Keyence, Essen, Germany) with a 20x magnification.

2.5. Thermal analysis

For thermogravimetric analysis (TGA) and derivative thermogravimetric analysis (DTG), ESC-OX was measured using a NETZSCH TG 209F1 Libra (NETSCH, Germany). The sample was placed in the form of powder in an 85 μL aluminium pan and was then heated from 35°C to 600°C with 10°C / min heating rate. The thermal decomposition was analyzed using NETZSCH Proteus Software. The experiments were carried out under nitrogen gas flow of 20 mL / min. Thermal analysis of ESC-OX starting material, related substances, physical mixtures, extrudates and tablets were performed using differential scanning calorimetry (DSC, DSC 1, Mettler-Toledo, Giessen, Germany). ESC-OX and related substances were heated at 10°C / min from 20°C to 200°C, whereas plasticizers, physical mixtures, extrudates, and tablets were heated over the temperature range of 20°C to 160°C.

2.6. X-ray diffractometer (XRD)

XRD analysis was carried out for starting materials, extrudates and tablets using a Rigaku Miniflex 300 diffractometer (Rigaku, Neu-Isenburg, Germany) in Θ/2Θ geometry at ambient temperature using Cu-Kα radiation (Θ = 1,54182 Å). The amperage was 15 mA and the voltage 40 kV. Scans were performed from 2θ = 2° to 50° with 0.01° step width. The scan resolution was 0.0025 and the scan speed 1.7°/min. The duration of each measurement was 30 min.

2.7. Polarized light microscopy

Microscopic images were taken using the light microscope DM LB (Leica Microsystems, Germany) with polarization filters with a 5x magnification. The raw materials ESC-OX and PEO were measured directly as powders, whereas for the extrudate and 3D printed tablet small pieces were examined.

2.8. FT-IR spectra measurements

FT-IR spectra measurements were performed to investigate possible interactions between the active ingredient ESC-OX and the polymers for all self-produced formulations. The raw materials were measured directly as powders, whereas for the extrudates and tablets, a small piece of each was cut using a scalpel. Infrared spectra were recorded with a Shimadzu IR Affinity-1 equipped with an ATR unit (Shimadzu, Germany).

2.9. Assay in extrudates, 3D printed tablets and in solution

A 3D printed tablet ($n = 3$, mean ± SD) or a section of a drug-loaded extrudate (approximately 0.1 g) ($n = 10$, mean ± SD) was placed in a 100 mL volumetric flask and dissolved in 100 mL of a mixture of methanol and 5 mM potassium dihydrogen phosphate buffer pH 3.8 (50/50, *V/V*). Samples of the solutions were then filtered through a 0.45 μm nylon filter. An Elite LaChrom system consisting of L-2200 automatic sampler, L-2130 high pressure pump, L-2300 column oven and L-2400 UV detector was used (all Hitachi-VWR, Darmstadt, Germany). Chromatographic separation of ESC-OX and related substances were carried out on an achiral XSelect CSH C18 column [3.0×150 mm, 3.5 μm (Waters, Germany)]. After injection of 20 μL sample solution the samples were separated with the aid of a gradient using a mobile phase of methanol and 5 mM potassium dihydrogen phosphate buffer pH 3.8 (Table 3). The flow rate was 0.7 mL/min and the column temperature was maintained at 45°C. The eluent was screened due to the absorption maximum at a wavelength of 239 nm. The run time was 30 min. The identification and quantification of ESC-OX and related substances were done with solutions of the USP reference standards. The solutions were also used for the determination of the selectivity. The limit of detection

Table 3

Gradient for the separation of ESC-OX and related substances.

Time (min)	Methanol (% *V/V*)	Buffer (% *V/V*)
0–3.0	30	70
3.0–5.0	30 → 35	70 → 65
5.0–24.0	35 → 40	65 → 60
24.0-25.5	40 → 95	60 → 5
25.5-27.5	95	5
27.5-27.6	95 → 30	5 → 70
27.6-30.0	30	70

(LOD) for ESC for the assay was determined to be 18.1 ng/mL and the limit of quantification (LOQ) to be 54.7 ng/mL. A LOD and LOQ for ESC of 19.4 ng/mL and 58.9 ng/mL were determined for the dissolution. Linearity was given for the assay of ESC in the concentration range of 60 to 140 µg/mL with an $R^2 > 0.999$, whereas for the dissolution linearity was given with an $R^2 > 0.999$ in the concentration range of 0.2-12 µg/mL. The accuracy of the content determination in the samples was verified by using USP reference standards. Precision, determined as repeatability, with a coefficient of variation of 0.78 % was determined for ESC.

To determine the stability of ESC-OX in solution, 100 mg ESC was dissolved in 100 mL 0.1 N hydrochloric acid, de-ionized water and 0.1 N sodium hydroxide and the content was also determined by HPLC at a wavelength of 240 nm.

2.10. Enantiomeric purity in extrudates, 3D printed tablets and in solution

A 3D printed tablet ($n = 3$, mean ± SD), a Cipralex® 10 mg film-coated tablet ($n = 3$, mean ± SD), or sections of a drug-loaded extrudate ($n = 10$, mean ± SD) (approximately 0.1 g) were placed in a 100 mL volumetric flask and were dissolved in 100 mL of a mixture of acetonitrile and potassium dihydrogen phosphate buffer pH 7.0 (15/85, *V/V*). In contrast, for the stability studies of ESC-OX in solution, such as on the achiral column, 100 mg ESC was dissolved in 100 mL 0.1 N hydrochloric acid, de-ionized water and 0.1 N sodium hydroxide. Samples of the solutions were then filtered through a 0.45 µm nylon filter. An Elite LaChrom system consisting of L-2200 automatic sampler, L-2130 high pressure pump, L-2300 column oven and L-2400 UV detector was used (all Hitachi-VWR, Darmstadt, Germany). Chromatographic separation was achieved according to the USP method of ESC-OX for "enantiomeric purity" on an Ultron ES-OVM column [4.6×150 mm, 5 µm (Shinwa Chemical Industries Ltd., Japan)]. The chiral column was additionally equipped with an Ultron ES-OVM holder, in which a guard cartridge with the dimensions 4.6×10 mm was integrated. The following chromatographic conditions as defined by the USP method were set: A mobile phase consisting of acetonitrile and potassium dihydrogen phosphate buffer pH 7.0 (15/85 *V/V*) was used. The flow rate was 0.6 mL/min and the column temperature was maintained at 25°C. After injection of 15 µL, the eluent was screened due to the absorption maximum at a wavelength of 240 nm. The run time was set to 25 min. The samples were analyzed after establishment of the method according to the USP method.

2.11. Mass spectrometry

A UHR-QTOF maXis 4G mass spectrometer (Bruker Daltonics, MA, USA) equipped with an ESI source was used in positive ionization mode to detect ESC and degradation products in alkaline solution. For this purpose, 127.8 mg ESC-OX, equal to 100 mg ESC, was dissolved in 100 mL 0.1 N sodium hydroxide solution and heated for 1 h and 12 h at 70°C respectively. The solutions were further diluted with methanol to achieve a target concentration of 100 µg/mL ESC. For the determination, the following mass spectrometric conditions were used: The capillary voltage was set to 4 kV and the temperature was adjusted to 180°C. The gas flow was 4.0 L/min and the nebulizer pressure was 0.3 bar. The monitored mass-to-charge range (m/z) was 50 to 1500 m/z and mass spectra were presented in the range of interest from 320 to 350 m/z.

2.12. Dissolution

In vitro drug release studies from ESC-OX tablets with a target mass of 10 mg ESC were carried out using dissolution tester AT7 Smart (Sotax, Aesch, Switzerland) with USP type I apparatus (basket) and USP type II apparatus (paddle) at 37°C ± 0.5°C with rotating speed of 75 rpm in 900 mL 0.1 N hydrochloric acid ($n = 3$, mean ± SD). Samples were withdrawn manually after 2 min, 5 min, 10 min, 15 min, 20 min, 30 min, 45 min, 60 min, 75 min, 90 min, 105 min and 120 min. The amount of ESC was quantified by HPLC. The eluent which was dissolved in the dissolution medium was analyzed with the above mentioned method for the content uniformity at the UV maximum of 238 nm.

3. Results

3.1. Hot-melt extrusion and 3D printing of tablets

Three formulations were selected with respect to temperature, physical properties of the polymers and printability for FDM 3D printing. For formulations F1 and F2, an extrusion temperature of 150°C was chosen to study the degradation of ESC-OX near the melting temperature. In addition, the influence of the additional amount of basic bPMMA in formulation F2 compared to formulation F1 containing only HPMC on degradation of ESC-OX was investigated. Therefore, it was clarified in greater detail whether the addition of the basic polymer bPMMA led to increased degradation of the base-labile active substance. From these investigations and after formulation development, formulation F3, designated as optimized formulation, represented the most suitable formulation, which could be extruded at the lowest possible extrusion temperature of 80°C and printed. Regarding the physical properties, changes in the solid-state of the crystalline ESC-OX starting material during both melting processes in extrudates and in 3D printed tablets were investigated. The degree to which ESC-OX existed in the crystalline state below the melting temperature and was amorphized by FDM 3D printing was examined. Furthermore, the printability was studied for the obtained extrudates of all three formulations from the extrusion process. All extrudates were sufficient flexible and could be successfully printed into 3D printed tablets with the help of the Prusa i3 Mk3 printer at a nozzle temperature of 180°C, which could be seen in the microscopic images (Fig. 2). The images of the 3D printed tablets showed the different texture of the tablets depending on the polymer and temperature used. All tablets were printed with a concentric infill (Fig. 2a-c). The tablets of the originator product Cipralex® 10 mg film-coated tablets are shown in Fig. 2d for comparison.

For the tablets of formulations F1 and F2 based on HPMC, higher print bed temperatures of 65°C were necessary to ensure sufficient adhesion of the layers to each other, but also to the print bed. As a result, the individual layers are more fused together and less recognisable (Fig. 2a and b). The tablets of formulation F3 based on bPMMA could be printed at a print bed temperature of 35°C. Due to the lower glass transition temperature of bPMMA (57°C vs. 115 ° for HPMC) (Parikh, et al. 2016; O'Donnell and Woodward 2015; Ilyés, et al. 2019), lower printing temperatures are sufficient to ensure complete solidification of the individual layers after the melting process. In addition, the concentric infill is clearly visible (Fig. 2c). The oval and white Cipralex® 10 mg film-coated tablet has a score, which allows the tablet to be divided into two equal halves. In addition, the tablets are marked on the front with "E" and "L" on each half of the score, which can be clearly seen in Fig. 2d.

3.2. Thermal analysis

3.3.1. Thermogravimetric analysis

TGA measurements confirmed that the degradation of ESC-OX took place in two consecutive events (Pinto et al., 2018; Akay et al., 2021). As already described by Pinto et al. (2018), the first major mass loss starting from the melt temperature of ESC-OX up to 237°C is related to the decomposition of the oxalate, whereas the second major mass loss up to 300°C is caused by the degradation of ESC (Pinto et al., 2018) (Fig. 3).

3.3.2. DSC analysis

DSC analysis of ESC-OX starting material showed an endothermic peak at approximately 153°C correlating to the melting temperature
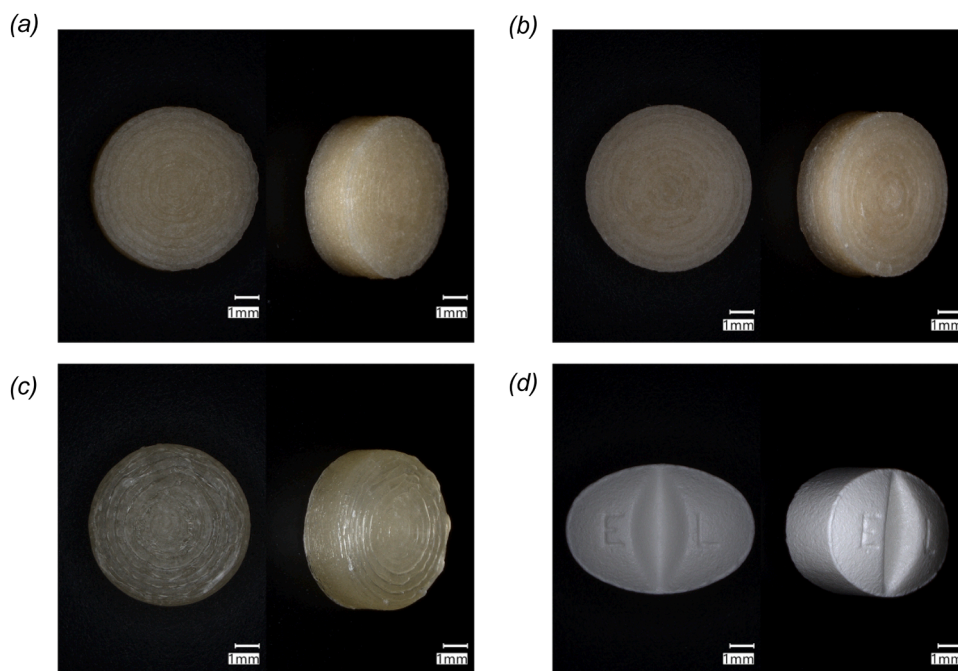
Fig. 2. Images of top and side view of the 3D printed tablets of formulation F1 (a), of formulation F2 (b), of formulation F3 (c) and Cipralex® 10 mg film-coated tablets (d) (scale bars: 1 mm).
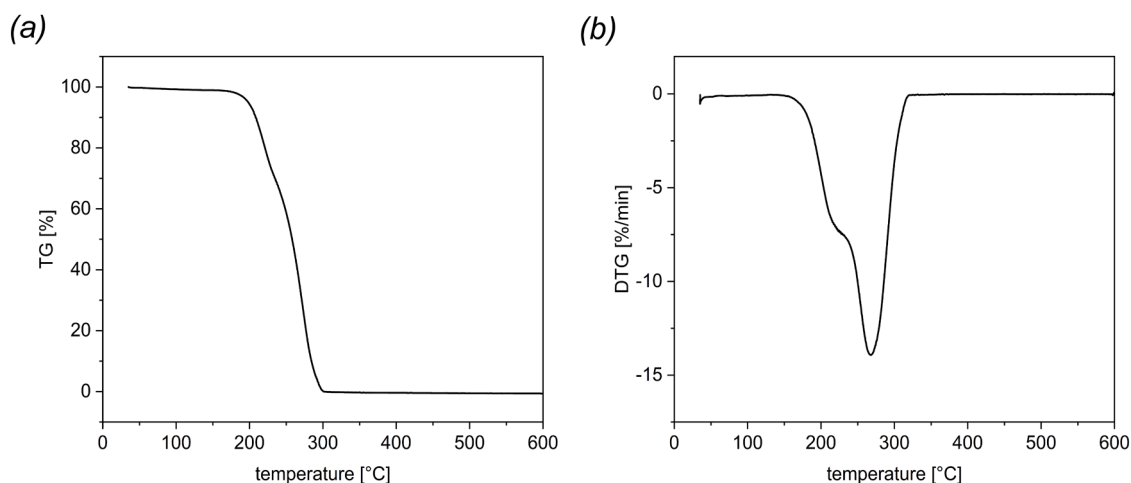

Fig. 3. TG (a) and DTG curves (b) of ESC-OX.

(Pinto et al., 2018) (Fig. 4a). In addition to the DSC thermogram of ESC-OX, the thermograms of the degradation products are also depicted in Fig. 4b, c and d.

The DSC thermogram for the impurity CIT-A showed an endothermic event at 126°C, whereas for the impurity CIT-B an onset could be observed at 107°C with an endothermic peak at 125°C. Finally, a higher melting point of 181°C with subsequent decomposition could be observed for CIT-C.

Furthermore, the melting behavior of R-Citalopram oxalate and the racemate citalopram hydrobromide was investigated (Fig. 5). For R-Citalopram oxalate, an endothermic peak at 149°C was observed (Fig. 5a). In contrast, a higher melting point of approximately 188°C was determined for the racemate citalopram hydrobromide (Fig. 5b), which is consistent with the observations of Pinto et al. (2018). This shows the higher stability of the racemate compared to the enantiomers, which was also described by De Diego et al. (2011) for the racemate present as an oxalate.

Additionally, the formulations with ESC-OX were examined. The physical mixtures of all formulations showed the endothermic event of ESC-OX at 153°C (Fig. 6a-c). Furthermore, endothermic peaks could be observed for polyethylene glycole (PEG) 6.000 and polyethylene oxide (PEO) which diffractograms are shown in the Fig. S1 of the Supplementary data. PEG 6.000 exhibited an endothermic event with an onset at 59.4°C and a peak at 63.6°C, whereas for the PEO an endothermic event with an onset at 62.4°C and a peak at 67.9°C could be observed. For formulation F1 and F2, which were extruded at a temperature of 150°C and printed at 180°C, the endothermic event of ESC-OX was not present in the extrudates and tablets. The absence of the endothermic event indicated that ESC-OX seems to be in amorphous form in the extrudates and 3D printed tablets of these formulations. For formulation F3, on the other hand, an endothermic event with an onset at 121.1°C and a peak at 136.5°C was observed in the extrudates from the extrusion process at 80°C, which could not be detected in the 3D printed tablets printed at 180°C (Fig. 6c). This indicated that ESC was crystalline in the
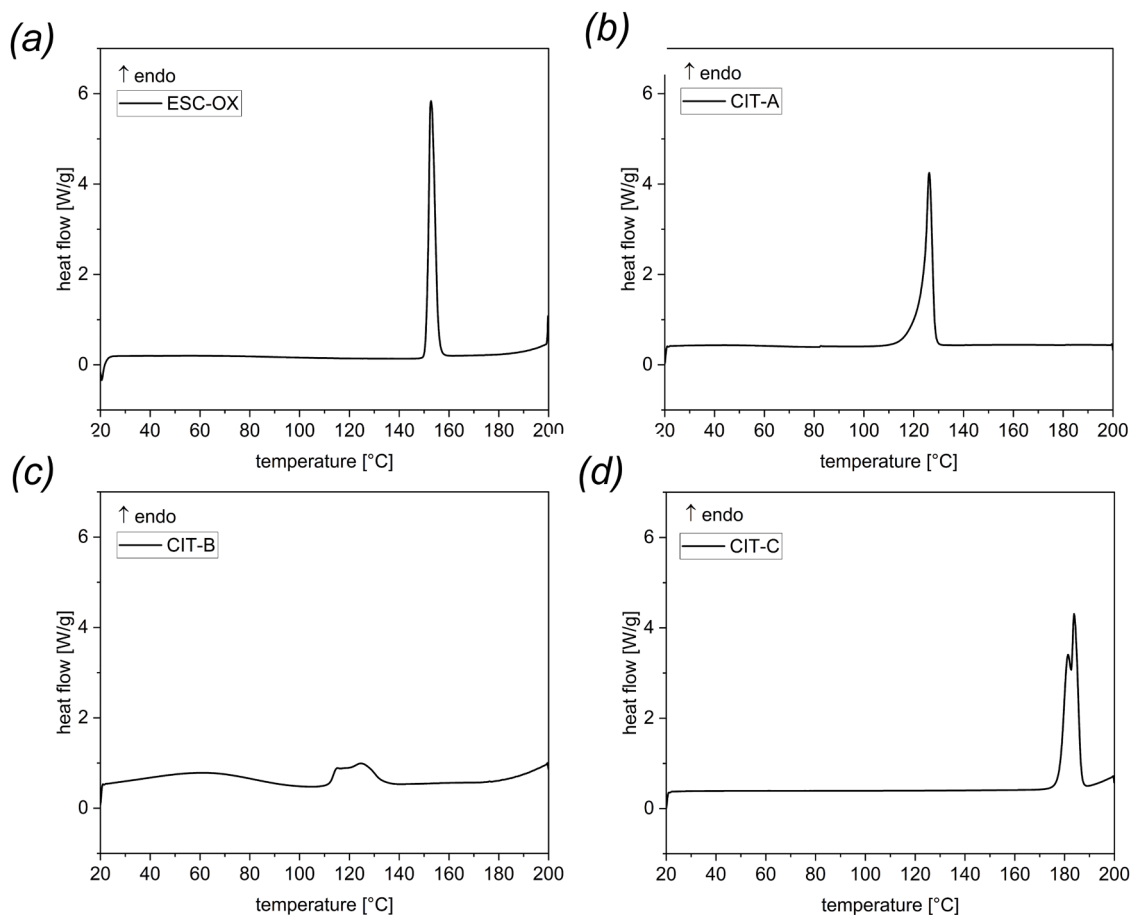
Fig. 4. DSC thermograms of ESC-OX (a), CIT-A (b), CIT-B (c) and CIT-C (d).
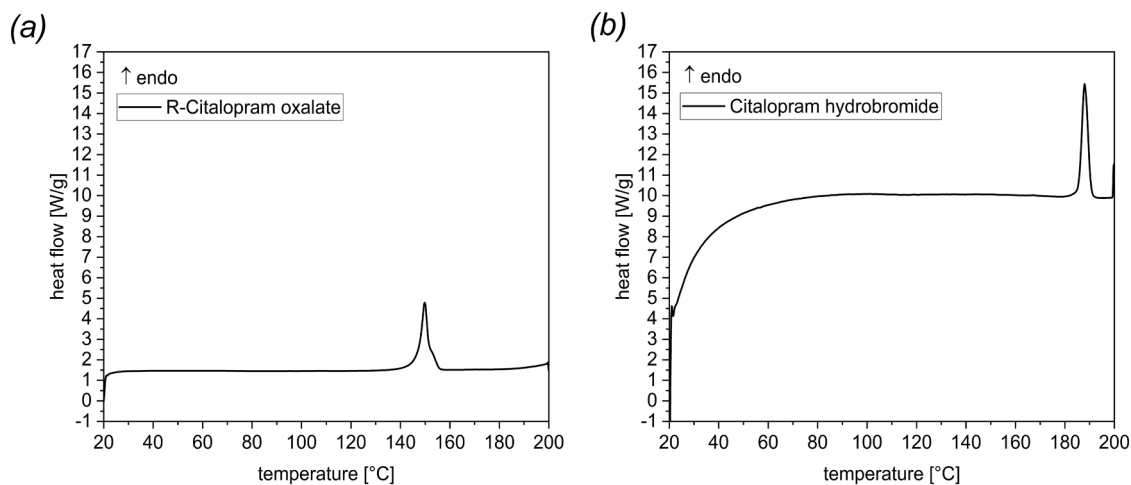

Fig. 5. DSC thermograms of R-Citalopram oxalate (a) and citalopram hydrobromide (b).

extrudates in the formulation F3 and was amorphized during the 3D printing process. The crystalline parts of the PEO in F3 were still visible in both the extrudates and the 3D printed tablets. The thermogram of the Cipralex® 10 mg film-coated tablets clearly showed the endothermic peak of ESC-OX at 152.4°C with an onset at 148.5°C, indicating the crystalline state (Fig. 6d). To confirm these observations, XRD analysis were conducted.

3.3. X-ray diffraction (XRD)

XRD analysis were performed to investigate the physical form of ESC-OX in the physical mixtures, extrudates and 3D printed tablets (Fig. 7). The typical diffraction peaks in the starting material of ESC-OX agreed with those of Alkahtani et al. (2021) at 13.14°, 13.16°, 16.06°, 19.2°, 20.94°, and 27.12°. While the physical mixtures showed the crystalline peaks of ESC-OX, the absence of these peaks in extrudates and 3D printed tablets of formulations F1 and F2 indicated the amorphous state
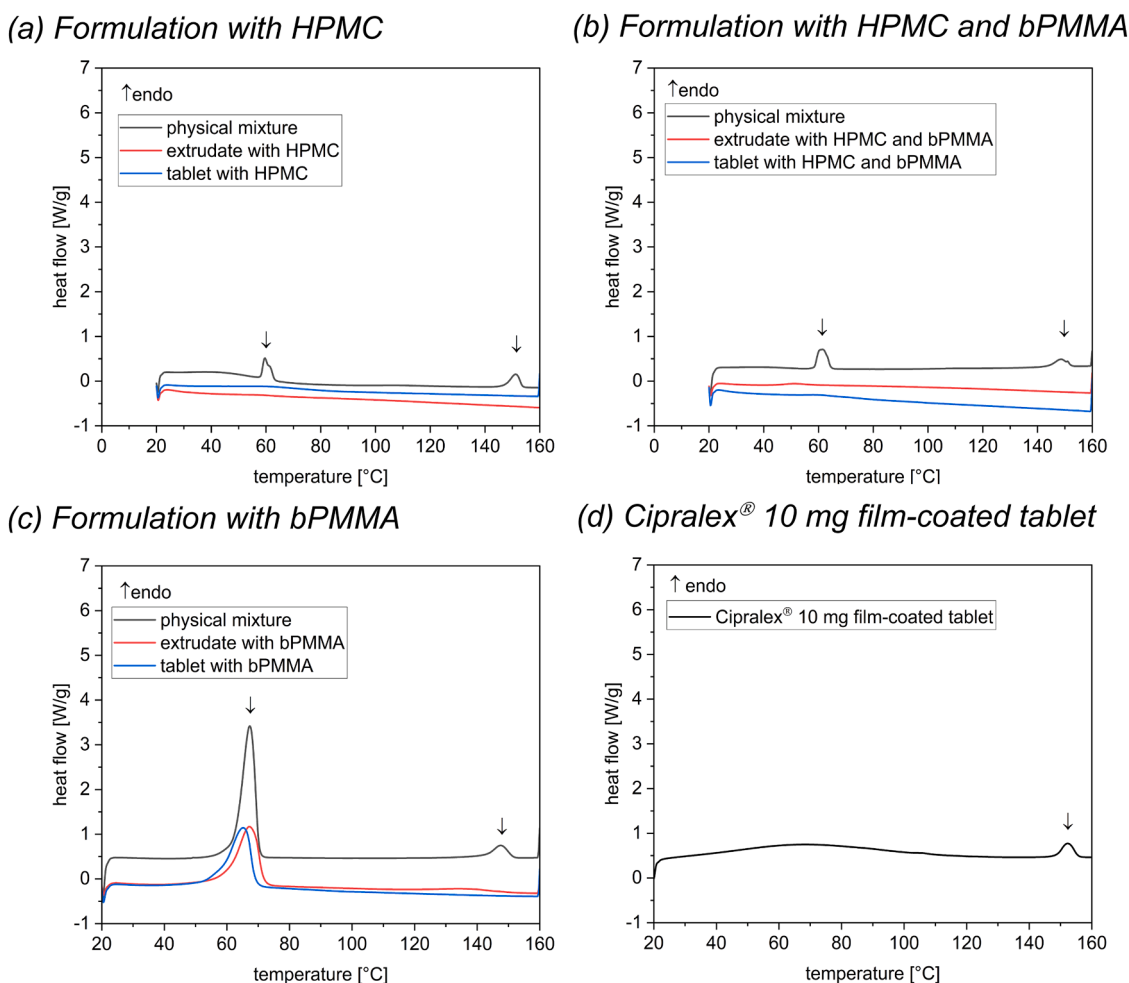
Fig. 6. DSC thermograms of formulation F1 (a), formulation F2 (b), formulation F3 (c) and Cipralex® 10 mg film-coated tablets (d), respectively.

of the drug and the production of amorphous solid dispersions (Fig. 7a and b). For formulation F3, on the other hand, characteristic peaks of ESC can still be observed in the extrudates, which were absent in the 3D printed tablets (Fig. 7c). Only the crystalline parts of PEO with characteristic peaks at 19.0° and 23.2°, marked with an arrow in Fig. 7c and depicted separately in Fig. S2 of the Supplementary Data, could still be seen in both, the extrudates and 3D printed tablets (Xu et al., 2012). This illustrates the possibility of *in-situ* amorphization of ESC-OX during FDM 3D printing and is shown in more detail in the diffractogram of Fig. 8. Furthermore, the results could be confirmed with polarization microscope images and were presented in Fig. S3 (Supplementary Data). Lastly, the Cipralex® 10 mg film-coated tablets were investigated and also showed crystalline peaks of ESC (Fig. 7d).

3.4. FT-IR spectra measurements

FT-IR spectroscopy was used to investigate potential interactions between ESC-OX and the polymers (Fig. 9). The FT-IR spectrum of ESC-OX showed characteristic bands at 2953 cm^{-1} (C–H stretching), 2231 cm^{-1} (C≡N stretching vibration) and 1221 cm^{-1} (C–N stretching) (Alkahtani et al., 2021; Song et al., 2016; Kumbhar, 2013). The polymer bPMMA showed characteristic bands for the dimethylamino groups at 2822 cm^{-1} and 2770 cm^{-1} (Evonik, Technical Information Eudragit® E 100, EUDRAGIT® E PO and EUDRAGIT® E 12,5., 2022). In addition, further characteristic peaks for the ester groups of bPMMA at 1267 cm^{-1}, 1238 cm^{-1} and 1144 cm^{-1} as well as the C=O ester vibration at 1724 cm^{-1} are also recognizable and in agreement with data from (Evonik, Technical Information Eudragit® E 100, EUDRAGIT® E PO and

EUDRAGIT® E 12,5., 2022). FT-IR spectrum of HPMC showed characteristic bands for the O–H stretching vibration at 3458 cm^{-1}, for the C–H stretching vibration in the range from 2800 cm^{-1} to 3000 cm^{-1} as well as for the C–O stretching vibration at 1047 cm^{-1}. Deformation vibrations are visible for the C–H group at 1454 cm^{-1} and for the O-H group at 1373 cm^{-1} (Furqan et al., 2017). No specific interactions between the active ingredient ESC-OX and the polymers could be detected.

3.5. Assay in solution

The content determination of ESC-OX on an achiral column in alkaline solution showed that ESC-OX is unstable at these conditions. After dissolving in 0.1 N NaOH and subsequent determination of the content of ESC, only 80.34 % ESC was present and impurity CIT-A was formed as the main degradation product. No instabilities were observed in acidic or neutral solution. The content in acidic solution was 103.63 %, while in neutral medium a content of 100.24 % was determined. These samples were also used to investigate the stability of ESC-OX in solution after 5 days on the chiral column. Furthermore, the stability of ESC-OX was also investigated when heating up the solution for 1 h at a temperature of 70°C, in order to accelerate the degradation (Fig. 10a).

Additional degradation of ESC-OX was evident in basic solution. After 1h at 70°C, only 29.78 % ESC was present. In addition to the degradation product CIT-A with a content of 64.44 %, another impurity with a content of 3.94 % was formed. The impurity was described in literature as citalopram carboxylic acid (Dhaneshwar, et al. 2008; Rao et al., 2008) and could be confirmed on the basis of the mass-to-charge range (m/z) of 344.17 with mass spectrometric measurements. The
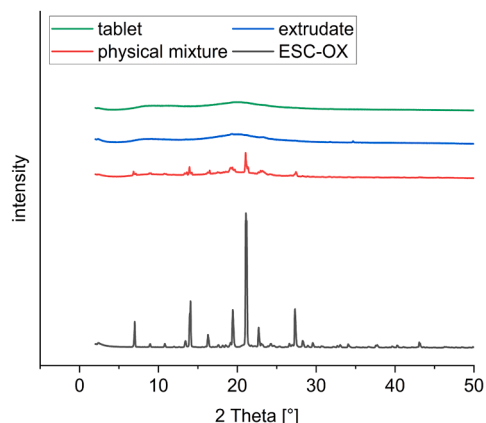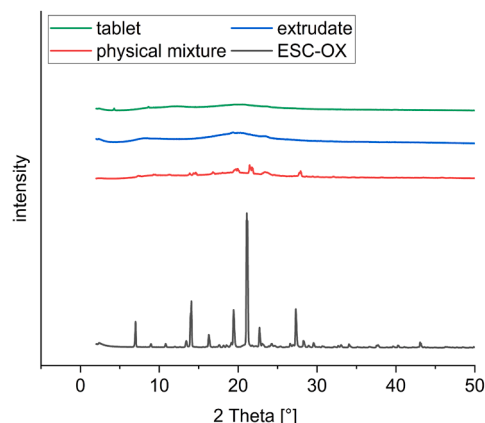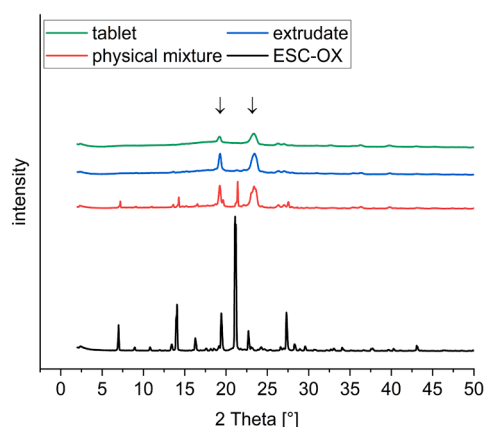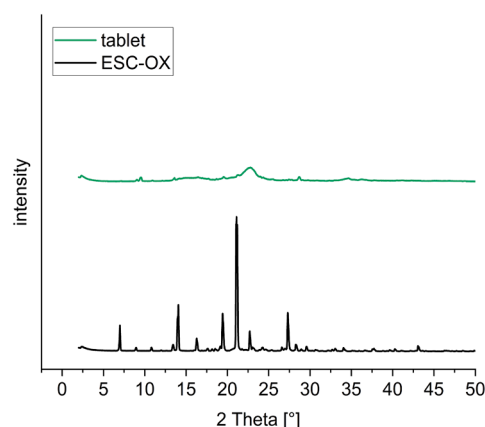
Fig. 7. X-ray diffractograms of formulation F1 (a), formulation F2 (b), formulation F3 (c) and Cipralex®10 mg film-coated tablets (d), respectively.
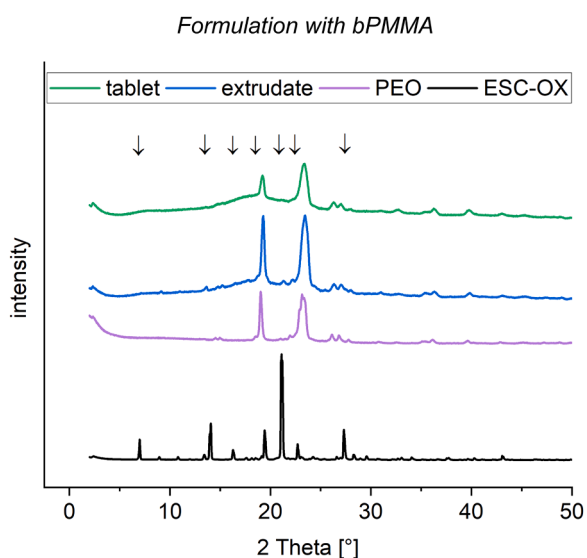

Fig. 8. X-ray diffractogram of ESC-OX, PEO, extrudate as well as 3D printed tablet of formulation F3.

content in acidic medium and also in water remained stable with 101.86 % and 101.06 %.

For further investigations, the samples were heated in 0.1 N NaOH for 12 h at a temperature of 70°C (Fig. 10b). After 12 h, the content of

ESC decreased further and only a small amount with 0.40 % ESC was present. CIT-A was formed with a content of 42.22 % and especially citalopram carboxylic acid originated to a higher content with 62.03 %, which was again conformed with mass spectrometric measurements. The obtained mass spectra and detailed explanations can be found in Fig. S4 of the Supplementary Data. Structural formulas of CIT-A and citalopram carboxylic acid are shown in Fig. 11a and b. Thus, the observations made on the instability of ESC in basic solution are consistent with the results of Dhaneshwar et al. (2008).

### 3.6. Assay in extrudates and 3D printed tablets

After the instability of ESC-OX in basic solution was confirmed, the thermal stress as well as the influence of different polymer matrices on the degradation of the active substance was investigated during hot-melt extrusion and FDM 3D printing on the achiral column. As a result, degradation of the active ingredient ESC-OX in the extrudates and 3D printed tablets could be observed and different degradation products were formed depending on the polymer matrix. For formulation F1 containing the polymer HPMC, the content in the extrudates after extrusion was 91.20 ± 0.71 %. After 3D printing, further minor degradation of the active ingredient was evident and a content of 89.65 ± 0.32 % ESC was found in the 3D printed tablets. Major degradation products in formulation F1 which could be identified were CIT-A, CIT-B and CIT-C which are shown in Fig. 11a as well as in Fig. 12a and b.

In the extrudates, the highest amount was found for CIT-C with 3.00 ± 0.18 % followed by CIT-A with a content of 1.41 ± 0.10 % and CIT-B with a content of 1.30 ± 0.19 %. In the 3D printed tablets, 2.73 ± 0.13 %

(a) Formulation with HPMC
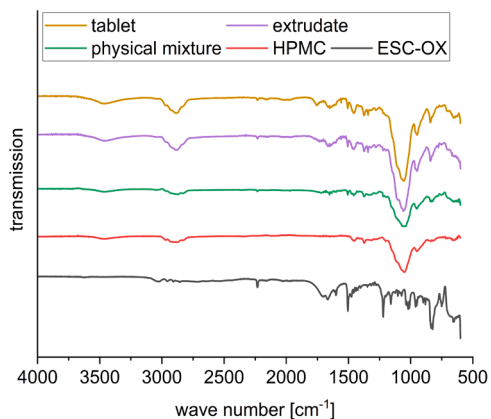
(b) Formulation with HPMC and bPMMA
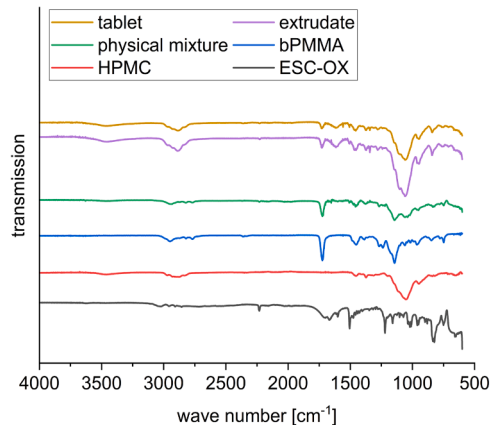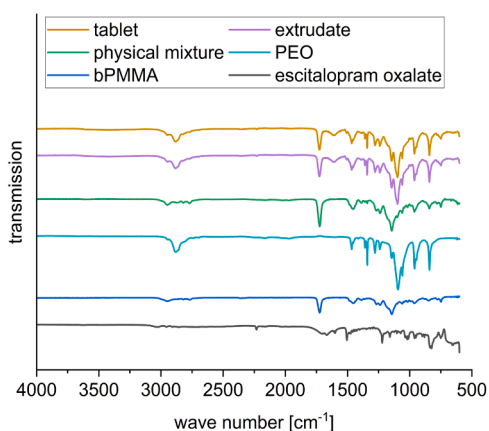

(c) Formulation with bPMMA

Fig. 9. FT-IR spectra of formulation F1 (a), formulation F2 (b) and formulation F3 (c), respectively.
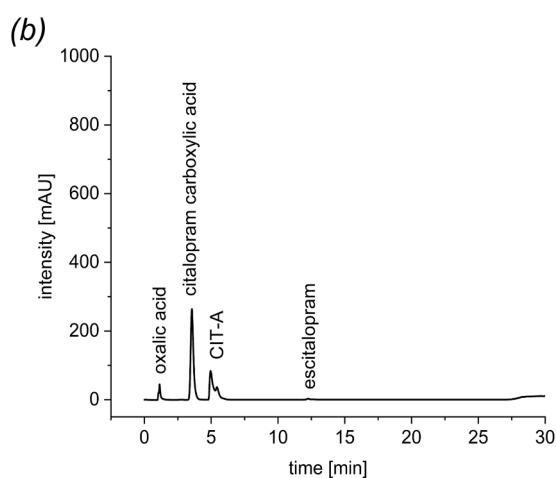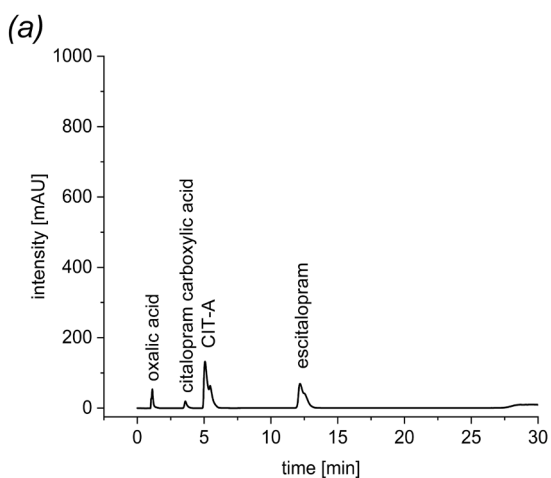

Fig. 10. HPLC chromatograms of ESC-OX in 0.1 N NaOH for 1 h at 70°C (a) and for 12 h at 70°C (b).

CIT-C, 2.04 ± 0.03 % CIT-A and 1.84 % $\pm$ 0.12 % CIT-B were formed. For formulation F2, which contains the polymers HPMC and bPMMA, a higher content of ESC was achieved compared to the first formulation extruded at the same temperature. The content in the extrudates of formulation F2 was 98.29 ± 2.67 % ESC and 1.70 ± 0.09 % CIT-A as the major degradation product. After 3D printing, the content of ESC decreases to 98.16 ± 1.11 % and 2.48 ± 0.09 % CIT-A was recovered besides low amounts of CIT-B and CIT-C. The optimized formulation F3

containing only bPMMA could be extruded at a temperature of 80°C. The content of ESC in the extrudates was 100.45 ± 1.21 % at 80°C. After FDM 3D printing at a temperature of 180°C, a content of 100.13 ± 0.52 % ESC and only 0.57 % $\pm$ 0.1 % CIT-A and 0.13 % $\pm$ 0.001 % CIT-C could be found in the 3D printed tablets. The content of the Cipralex® 10 mg film-coated tablets on the market was also examined and a content of 104.09 ± 0.14 % was determined. No degradation products were detected in the tablets.
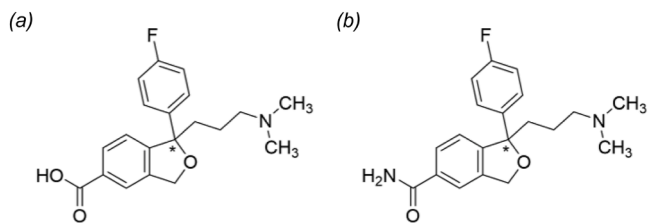
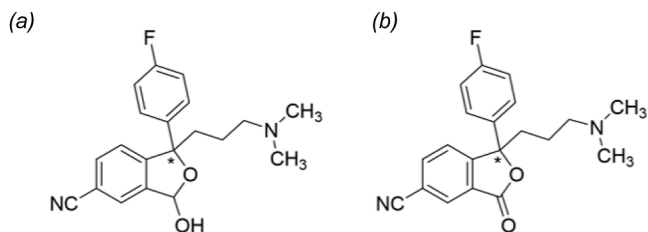**Fig. 11.** Structural formulas of citalopram carboxylic acid (a) and CIT-A (b)

Fig. 12. Structural formulas of CIT-B (a) and CIT-C (b).

3.7. Enantiomeric purity in solution

The stability of ESC was also examined in different solvents on a chiral column. The investigations in different solvents and after several days, showed that no conversion to the R-enantiomer could be observed. As already on the achiral column, only the instability in basic medium could be identified (Fig. 13a). An increase in degradation could be seen over time, which could be established in the analyzed samples after 5 days (Fig. 13b).

Initially, a content of 85.43 % ESC in 0.1 N sodium hydroxide was found and 13.33 % CIT-A was formed. The content of R-citalopram in the basic solution was 0.62 %. As on the achiral column, no instability could be noted in acidic and neutral solution. The content was 103.62 % ESC in 0.1 N hydrochloric acid and 102.73 % in water. In contrast, a content of 0.57 % R-citalopram was determined in acidic solution and 0.63 % in neutral solution. After five days, a further reduction of the content of ESC was visible in 0.1 N sodium hydroxide. The content in 0.1 N sodium hydroxide was 48.99 % ESC and the impurities CIT-A with a content of 47.74 % and also the citalopram carboxylic acid with a content of 3.61 % were formed. The content of R-citalopram did not change and was 0.62 %.

3.8. Enantiomeric purity in extrudates and 3D printed tablets

In addition to the degradation of the drug, the potential conversion into the R-enantiomer was also investigated during the production of extrudates and 3D printed tablets on the chiral column. For this purpose, the extrudates of the optimized formulation F3 (extrusion temperature of 80°C) as well as the corresponding 3D printed tablets were examined. In addition, the Cipralex® 10 mg film-coated tablets on the market were also analyzed (Fig. 14).

The content of ESC in the extrudates was 98.74 ± 1.63 % after extrusion. After FDM 3D printing, the content amounts to 97.08 ± 0.58 %. For R-Citalopram, the content was 0.73 ± 0.01 % in the extrudates and 0.69 ± 0.04 % in the 3D printed tablets compared to 0.60 ± 0.03 % which was already contained in ESC starting material. Therefore, it can be concluded that also during heat intensive processes no racemization takes place. The limits of the USP are met with a maximum of 3 % R-Citalopram. In addition to the self-produced extrudates and tablets, the Cipralex® 10 mg film-coated tablets on the market were analyzed. A content of 104.76 ± 4.00 % ESC was detected in the tablets. In contrast, 1.24 ± 0.06 % R-Citalopram was present and the maximum permissible amount was not exceeded either.

3.9. Dissolution

In addition to the content, the release behavior of ESC from the bPMMA tablets extruded at 80°C with 100 % infill was investigated and compared to the commercial product Cipralex® 10 mg film-coated tablets (Fig. 15). The USP monograph for ESC-OX tablets specified that at least 80 % ESC has to be released in 30 min in the paddle apparatus (USP II method) in 0.1 N hydrochloric acid at a rotational speed of 75 rpm. For the commercial product, it could be observed that after 30 min 95.11 ± 1.84 % ESC was released. Therefore, the requirements of the pharmacopoeia were met. Extrudates and 3D printed tablets floated on the surface of the dissolution medium and the basket apparatus was used for dissolution testing. The commercial product was also tested with the basket apparatus and it was observed that the complete active ingredient was released within two minutes (102.53 ± 6.43 %).

For extrudates and 3D printed tablets the release was slower. After 30 min, 97.84 ± 1.06 % ESC was released from the extrudates, whereas 80.66 ± 4.65 % ESC was released from the 3D printed tablets. The faster drug release from the extrudates in comparison to the 3D printed tablets can be explained by the larger surface area to volume ratio of the extrudates, which was already observed by Manini et al. (2022). But still, after 90 min, the active ingredient was completely released from both the extrudates and the 3D printed tablets (100.45 ± 5.15 % vs.
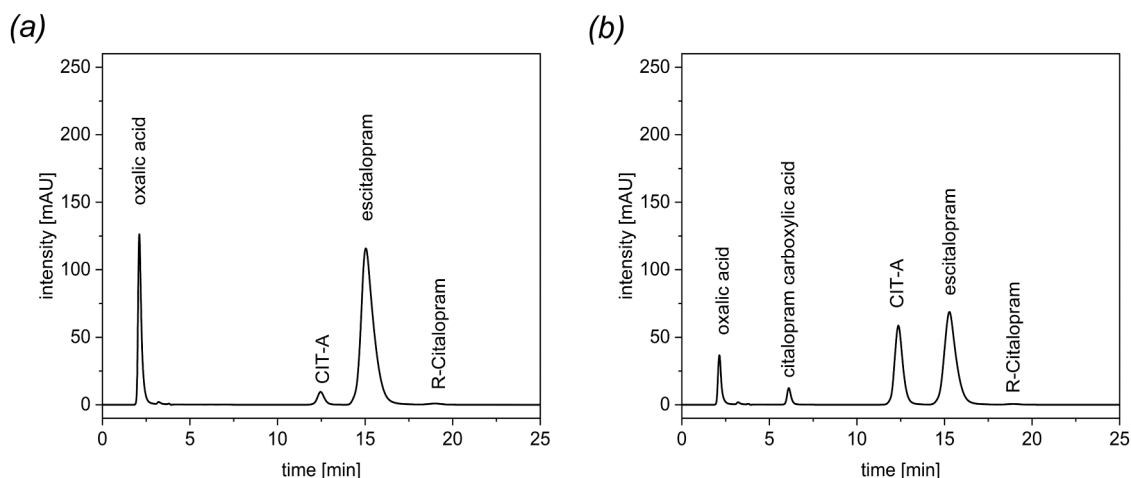

Fig. 13. HPLC chromatograms of ESC-OX in 0.1 N NaOH (a) and after 5 days (b).
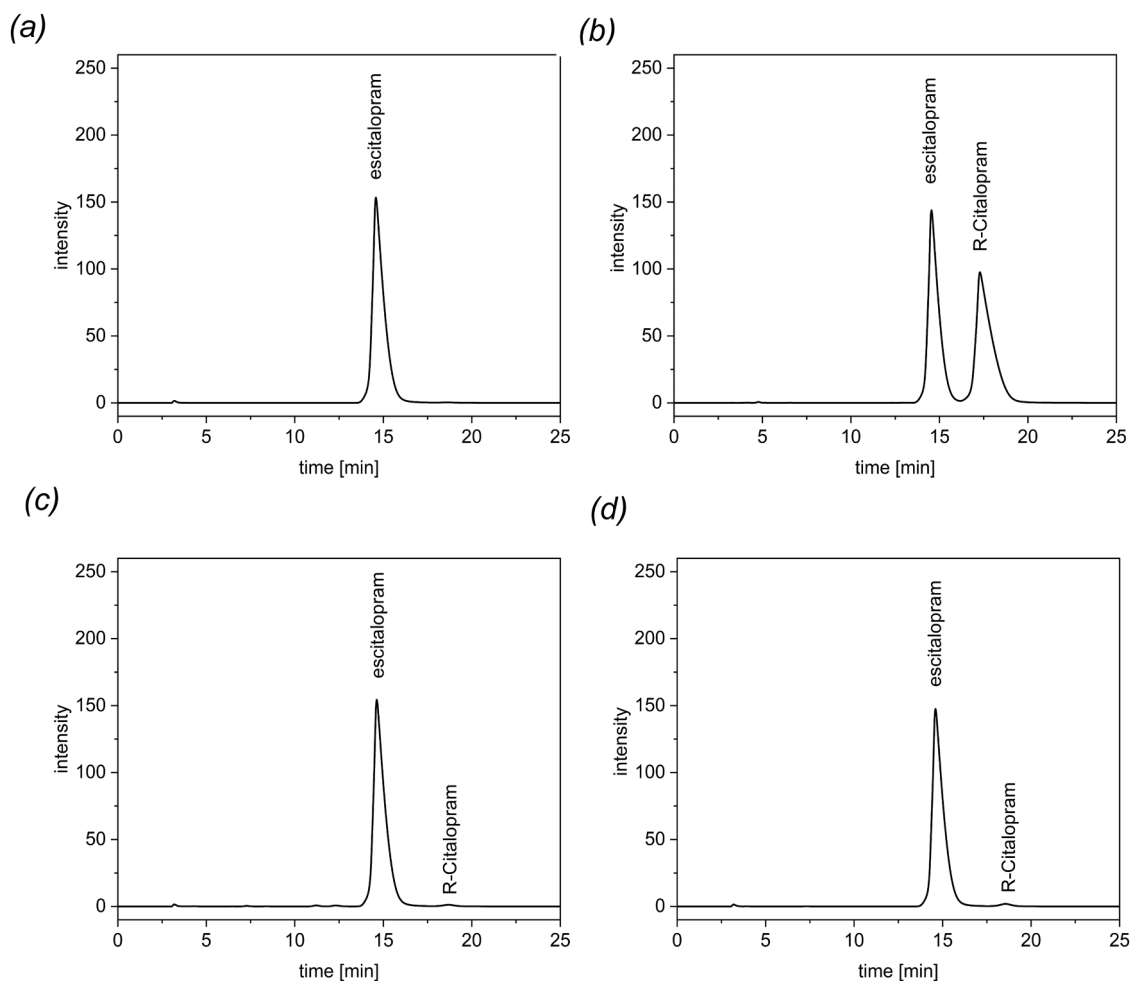
Fig. 14. HPLC chromatograms of ESC-OX (a), citalopram hydrobromide (b), the 3D printed tablet of F3 (c) and the Cipralex® 10 mg film-coated tablet (d).
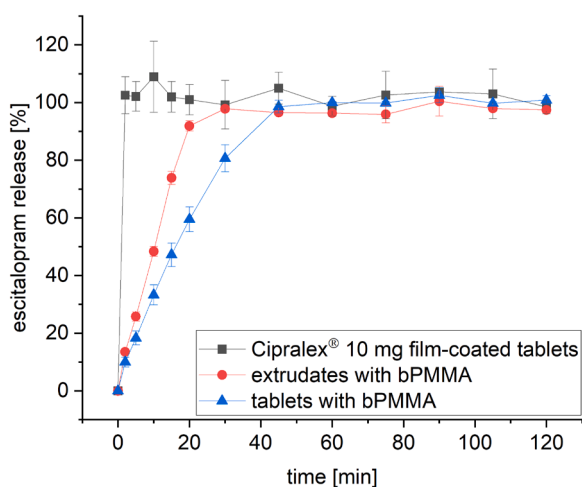

Fig. 15. In vitro dissolution profiles of ESC from bPMMA extrudates and tablets ($n = 3$) as well as from the commercial product Cipralex® 10 mg film-coated tablets, pH 1.2 buffer solution, USP Apparatus 1 (basket), 37 ± 0.5°C, 75 rpm.

102.52 ± 2.59 %). Regarding the differences in physical state, no slower release from the crystalline extrudates could be observed compared to the amorphous 3D printed tablets.

4. Discussion

Prepared extrudates and 3D printed tablets of three different formulations containing the active ingredient ESC-OX were investigated with regard to the physical state of ESC-OX. DSC and XRD results showed that amorphous solid dispersions could be prepared after hot-melt extrusion from formulations F1 and F2 with HPMC as main polymer. In these investigations it was found that amorphization of ESC-OX already took place below the melting temperature at 150°C and thus sufficient energy was present to enable conversion of ESC-OX from the crystalline state to the amorphous state during hot-melt extrusion. Also after FDM 3D printing at 180°C the drug remained in its amorphous form in both formulations F1 and F2. In contrast, for formulation F3 *in situ* amorphization of ESC-OX from crystalline extrudates with bPMMA was observed during FDM 3D printing. ESC-OX is still in its crystalline form in the extrudates of F3 due to hot-melt extrusion at only 80°C, far below the melting temperature. 3D printing takes place at 180°C, a temperature sufficient for the conversion from the crystalline state to the amorphous state of ESC-OX. *In-situ* amorphization is confirmed by DSC, XRD and polarized light microscopy. The crystalline parts of the semi-crystalline polymer PEO are still visible in extrudate and in small traces in the 3D printed tablet of F3. The phenomenon of *in-situ* amorphization can be of particular importance for production of customized dosage forms shortly before application, as stability of the amorphous form has only to be ensured until administration. The *in-situ* amorphization of drugs is not only relevant in FDM 3D printing. Also for the production of conventional dosage forms, e.g., tablets, *in situ* amorphization is researched. Approaches to achieve *in-situ*

amorphization in conventionally produced tablets using microwave radiation have been investigated in detail. For example, tablets with indomethacin and polyvinylpyrrolidone K12 were prepared and the influence of moisture content and energy input on the degree of amorphization were investigated. It was found that up to 80 % indomethacin could be amorphized within the tablet (Doreth et al., 2017). *In situ* amorphization allows the preparation and administration even of unstable amorphous forms that were not accessible with traditional approaches.

Dissolution studies of ESC-OX from the crystalline bPMMA extrudates and the amorphous 3D printed bPMMA tablets revealed a faster drug release from the extrudates. This suggests that the larger surface area to volume ratio of the extrudates (S/V = 2.4) compared to the 3D printed tablets (S/V = 1.4) has a greater influence on the release of ESC than the solid state of the drug. In addition, a slower release of the 3D printed tablets was also observed compared to the commercial product Cipralex®. This can be explained by the higher density of the 3D printed tablet. FDM printed dosage forms are very compact and have either very low or no porosity, which reduces the surface area exposed to the dissolution medium drastically and further delays the drug release.

Due to the pronounced instability of ESC-OX in basic solution, the degradation of the active ingredient and the formation of degradation products in the extrudates and 3D printed tablets were studied using HPLC. Purity tests showed that the polymer matrix can have a decisive influence on the degradation products of ESC. In formulation F1 with the polymer HPMC, CIT-C was formed to the greatest extent, while in formulation F2 with the combination of HPMC and bPMMA, CIT-A was formed to the greatest extent. Formulation F3, which did not contain HPMC and consisted of the polymer bPMMA as matrix, CIT-A was also the main degradation product, but only in comparably small quantities. Regarding the amount of degradation, less degradation of ESC-OX was observed in F2 compared to F1 despite the additional amount of the basic polymer bPMMA. F3 with bPMMA as the main polymer even represented the formulation with the highest content of ESC and lowest degradation. This illustrates that despite the use of a basic matrix polymer (bPMMA), processing in the melt and thus the absence of water could significantly reduce degradation of ESC. This is further supported by long term stability data after 6 months. Stored at atmospheric conditions for 6 months, 101.91 ± 0.77 % were recovered. With respect to enantiomeric purity, both temperature and pH of the solution do not appear to affect the conversion of the S-enantiomer to the R-enantiomer. No formation of the R-enantiomer could be observed, indicating sufficient stability of the S-enantiomer ESC-OX.

5. Conclusion

The obtained results showed that three formulations with the antidepressant ESC-OX could be hot-melt extruded and FDM 3D printed. The formulation F3 with bPMMA enabled *in-situ* amorphization from crystalline extrudates during FDM 3D printing which could be of decisive advantage, especially regarding their storage stability and clinical application. Thus, 3D printed tablets could be produced from stable extrudates according to the patient's needs just before application. Furthermore, formulation F3 with bPMMA showed no degradation of the active ingredient in the extrudates and only minor degradation in the 3D printed tablets. A possible racemization of the S-enantiomer into the R-enantiomer in formulation F3 could also be excluded. The dissolution of F3 extrudates and 3D printed tablets showed a fast drug release. Although ESC-OX was present in the extrudates in crystalline form, a rapid release of the active substance was achieved. The faster release compared to the tablets could be explained by the larger surface area to volume ratio. The slower release of the produced 3D printed tablets compared to the Cipralex® 10 mg film-coated tablets showed one of the hurdles of FDM 3D printing which can still be improved in the future.

Our study aimed to demonstrate the possibilities of formulation development, which on the one hand enabled *in-situ* amorphization of

ESC-OX during FDM 3D printing, but also made it possible to avoid the degradation of the thermally unstable drug almost completely. Besides the content determination on an achiral column, to our knowledge, this was the first study that investigated the behavior of an enantiomer during hot-melt extrusion and FDM 3D printing compared to the stability in solution and analyzed the content of the active ingredient by using a chiral column.

CRediT authorship contribution statement

Lena Hoffmann: Conceptualization, Data curation, Formal analysis, Investigation, Methodology, Visualization, Writing – original draft, Writing – review & editing. **Jörg Breitkreutz:** Conceptualization, Funding acquisition, Project administration, Resources, Supervision, Writing – review & editing. **Julian Quodbach:** Conceptualization, Funding acquisition, Project administration, Resources, Supervision, Writing – review & editing.

Data availability

Data will be made available on request.

Supplementary materials

Supplementary material associated with this article can be found, in the online version, at doi:10.1016/j.ejps.2023.106423.

References

Abdella, S., Youssef, S.H., Afinjuomo, F., Song, Y., Fouladian, P., Upton, R., Garg, S., 2021. 3D Printing of thermo-sensitive drugs. Pharmaceutics 13 (9), 1524.

Akay, S., Yang, Y., Kayan, B., 2021. Investigation on the solubility of the antidepressant drug escitalopram in subcritical water. J. Chem. Eng. Data. 66 (6), 2550–2560.

Alhnan, M.A., Okwuosa, T.C., Sadia, M., Wan, K.-W., Ahmed, W., Arafat, B., 2016. Emergence of 3D printed dosage forms: opportunities and Challenges. Pharm. Res. 33 (8), 1817–1832.

Alkahtani, M.E., Aodah, A.H., Abu Asab, O.A., Basit, A.W., Orlu, M., Tawfik, E.A., 2021. Fabrication and characterization of fast-dissolving films containing escitalopram/quetiapine for the treatment of major depressive disorder. Pharmaceutics 13 (6), 891.

Awad, A., Trenfield, S.J., Goyanes, A., Gaisford, S., Basit, A.W., 2018. Reshaping drug development using 3D printing. Drug Discov. Today. 23, 1547–1555.

Cipriani, A, Furukawa, T.A., Salanti, G., et al., 2009. Comparative efficacy and acceptability of 12 new-generation antidepressants: a multiple-treatments meta-analysis. Lancet 373 (9665), 746–758.

Cipriani, A., Santilli, C., Furukawa, T.A., et al., 2009. Escitalopram versus other antidepressive agents for depression. Cochrane Database Syst Rev, CD006532.

De Diego, H.L., Bond, A.D., Dancer, R.J., 2011. Formation of solid solutions between racemic and enantiomeric citalopram oxalate. Chirality 23 (5), 408–416.

Dhaneshwar, S.R., Mahadik, M.V., Kulkarni, M.J., 2008. Column liquid chromatography-ultraviolet and column liquid chromatography/mass spectrometry evaluation of stress degradation behavior of escitalopram oxalate. J AOAC Int 92, 138–147.

Doreth, M., Hussein, M.A., Priemel, P.A., Grohganz, H., Holm, R., de Diego, H.L., Rades, T., Löbmann, K., 2017. Amorphization within the tablet: Using microwave irradiation to form a glass solution in situ. Int. J. Pharm. 519 (1-2), 343–351.

Douroumis, D., 2012. Hot-Melt Extrusion: Pharmaceutical Applications. Wiley Online Library.

El Aita, I., Ponsar, H., Quodbach, J., 2018. A critical review on 3D-printed dosage forms. Curr. Pharm. Des. 24 (42), 4957–4978.

Evonik, Technical Information Eudragit® E 100, EUDRAGIT® E PO and EUDRAGIT® E 12,5. www.pharmaexcipients.com/wp-content/uploads/attachments/TI-EUDRAGIT-E-100-E-PO-E-12-5-EN.pdf?t=1508413942 (Accessed 22 November 2022).

Fernandez-Garcia, R., Prada, M., Bolas-Fernandez, F., Ballesteros, M.P., Serrano, D.R., 2020. Oral fixed-dose combination pharmaceutical products: industrial manufacturing versus personalized 3d printing. Pharm. Res. 37, 132.

Furqan, M., Iqbal, F., Tulain, R., 2017. Microwave radiation induced synthesis of hydroxypropyl methylcellulose-graft-(polyvinylalcohal-co-acrylic acid) polymeric network and its in vitro evaluation. Acta Pol. Pharm. 74, 527–541.

Gartlehner, G, Hansen, R.A., Morgan, L.C., Thaler, K., Lux, L., Van Noord, M., Mager, U., Thieda, P., Gaynes, B.N., Wilkins, T., Strobelberger, M., Lloyd, S., Reichenpfader, U., Lohr, K.N., 2011. Comparative benefits and harms of second-generation antidepressants for treating major depressive disorder: an updated meta-analysis. Ann. Intern. Med. 155 (11), 772–785.

Goyanes, A., Buanz, A.B., Hatton, G.B., Gaisford, S., Basit, A.W., 2015. 3D printing of modified-release aminosalicylate (4-ASA and 5-ASA) tablets. Eur. J. Pharm. Biopharm. 89, 157–162.

Goyanes, A., Scarpa, M., Kamlow, M., Gaisford, S., Basit, A.W., Orlu, M., 2017. Patient acceptability of 3D printed medicines. Int. J. Pharm. 530 (1), 71–78.

Grohganz, H., Löbmann, K., Priemel, P., Jensen, K.T., Graeser, K, Strachan, C, Rades, T., 2013. Amorphous drugs and dosage forms. J. Drug Deliv. Sci. Technol. 23, 403–408.

Hiew, T.N., Zemlyanov, D.Y., Taylor, L.S., 2022. Balancing solid-state stability and dissolution performance of lumefantrine amorphous solid dispersions: the role of polymer choice and drug-polymer interactions. Mol. Pharm. 19, 392–413.

Hoffmann, L., Breitkreutz, J., Quodbach, J., 2022a. Fused deposition modeling (FDM) 3D printing of the thermo-sensitive peptidomimetic drug enalapril maleate. Pharmaceutics 14 (11), 2411.

Hoffmann, L., Breitkreutz, J., Quodbach, J., 2022b. Hot-melt extrusion of the thermo-sensitive peptidomimetic drug enalapril maleate. Pharmaceutics 14 (10), 2091.

Holm, T.P., Kokott, M., Knopp, M.M., Boyd, B.J., Berthelsen, R., Quodbach, J., Löbmann, K., 2022. Development of a multiparticulate drug delivery system for in situ amorphization. Eur. J. Pharm. Biopharm. 180, 170–180.

Ilyés, K., Kovács, N.K., Balogh, A., Borbás, E., Farkas, B., Casian, T., Marosi, G., Tomut, ă I, Nagy, Z.K., 2019. The applicability of pharmaceutical polymeric blends for the fused deposition modelling (FDM) 3D technique: material considerations–printability– process modulation, with consecutive effects on in vitro release, stability and degradation. Eur. J. Pharm. Sci. 129, 110–123.

Institute of Health Metrics and Evaluation. Global Health Data Exchange (GHDx). https://vizhub.healthdata.org/gbd-results/ (Accessed 22 November 2022).

Jagtap, A, Bhaskar, M., 2013. Evaluation of antidepressant and antinociceptive activity of escitalopram. Ind. J. Pharm. Edu. Res. 47, 97–102.

Kalepu, S., Nekkanti, V., 2015. Insoluble drug delivery strategies: review of recent advances and business prospects. Acta Pharm. Sin. B. 5, 442–453.

Kanaujia, P., Poovizhi, P., Ng, W.K, Tan, R.B.H., 2015. Amorphous formulations for dissolution and bioavailability enhancement of poorly soluble APIs. Powder Technol 285, 2–15.

Kempin, W., Domsta, V., Brecht, I., Semmling, B., Tillmann, S., Weitschies, W., Seidlitz, A., 2018. Development of a dual extrusion printing technique for an acid- and thermo-labile drug. Eur. J. Pharm. Sci. 123, 191–198.

Khalid, G.M., Billa, N., 2022. Solid dispersion formulations by FDM 3D printing - a review. Pharmaceutics 14 (4), 690.

Kirino, E., 2012. Escitalopram for the management of major depressive disorder: a review of its efficacy, safety, and patient acceptability. Patient Prefer. Adher. 6, 853–861.

Kollamaram, G., Croker, D.M., Walker, G.M., Goyanes, A., Basit, A.W., Gaisford, S., 2018. Low temperature fused deposition modeling (FDM) 3D printing of thermolabile drugs. Int. J. Pharm. 545 (1–2), 144–152.

Konta, A.A., Garcia-Pina, M., Serrano, D.R., 2017. Personalised 3D printed medicines: which techniques and polymers are more successful? Bioengineering 4, 79.

Krause, J., Müller, L., Sarwinska, D., Seidlitz, A., Sznitowska, M., Weitschies, W., 2021. 3D printing of mini tablets for pediatric use. Pharmaceuticals 14, 143.

Kumbhar, M.S., 2013. Enhancement of solubility and dissolution rate of escitalopram oxalate by liquisolid compact technology. Int. J. Pharm. Chem. Sci. 2, 2277–5005.

Manini, G., Benali, S., Mathew, A., Napolitano, S., Raquez, J.-M., Goole, J., 2022. Paliperidone Palmitate as model of heat-sensitive drug for long-acting 3D printing application. Int. J. Pharm., 121662

O'Donnell, J.M., Shelton, R.C., 2015. Drug therapy of depression and anxiety disorders. In: Brunton, L.L., Chabner, B.A., Knollmann, B.C. (Eds.), Goodman & Gilman's: The Pharmacological Basis of Therapeutics, 12th ed. McGraw Hill https://accesspharmacy.mhmedical.com/content.aspx?bookid=1613&sectionid=102158640. (Accessed 20 November 2022).

O'Donnell, K.P., Woodward, W.H.H., 2015. Dielectric spectroscopy for the determination of the glass transition temperature of pharmaceutical solid dispersions. Drug Dev. Ind. Pharm. 41 (6), 959–968.

Parikh, T., Gupta, S.S., Meena, A., Serajuddin, A.T., 2016. Investigation of thermal and viscoelastic properties of polymers relevant to hot melt extrusion-III: Polymethacrylates and polymethacrylic acid based polymers. J. Excip. Food Chem. 5, 1003.

Pawar, J., Tayade, A, Gangurde, A., Moravkar, K., Amin, P., 2016. Solubility and dissolution enhancement of efavirenz hot melt extruded amorphous solid dispersions using combination of polymeric blends: a QbD approach. Eur. J. Pharm. Sci. 88, 37–49.

Pinto, B.V., Ferreira, A.P.G., Cavalheiro, E.T.G., 2018. Thermal degradation mechanism for citalopram and escitalopram. J. Therm. Anal. Calorim. 133 (3), 1509–1518.

Rao, R.N., Raju, A.N., Narsimha, R., 2008. Isolation and characterization of degradation products of citalopram and process-related impurities using RP-HPLC. J. Sep. Sci. 31 (10), 1729–1738.

Santomauro, D.F., Mantilla Herrera, A.M., Shadid, J., Zheng, P., Ashbaugh, C., Pigott, D. M., et al., 2021. Global prevalence and burden of depressive and anxiety disorders in 204 countries and territories in 2020 due to the COVID-19 pandemic. Lancet 398 (10312), 1700–1712.

Scoutaris, N., Ross, S.A., Douroumis, D., 2018. 3D Printed "Starmix" drug loaded dosage forms for paediatric applications. Pharm. Res. 35, 34.

Song, T., Quan, P., Xiang, R., Fang, L., 2016. Regulating the skin permeation rate of escitalopram by ion-pair formation with organic acids. AAPS PharmSciTech 17, 1267–1273.

Tan, D.K., Davis, D.A., Miller, D.A., et al., 2020. Innovations in thermal processing: hot-melt extrusion and KinetiSol® dispersing. AAPS PharmSciTech 21, 312.

Varghese, R., Sood, P., Salvi, S., Karsiya, J., Kumar, D., 2022. 3D printing in the pharmaceutical sector: advances and evidences. Sens. Int. 3, 100177.

Wang, N., Shi, H., Yang, S., 2022. 3D printed oral solid dosage form: Modified release and improved solubility. J. Control. Release. 351, 407–431.

Waugh, J., Goa, K.L., 2003. Escitalopram: a review of its use in the management of major depressive and anxiety disorders. CNS Drugs 17, 343–362.

WHO Model List of Essential Medicines—22nd list. 2021. https://www.who.int/publications/i/item/WHO-MHP-HPS-EML-2021.02 (Accessed 20 October 2022).

Windolf, H., Chamberlain, R., Breitkreutz, J., Quodbach, J., 2022. 3D Printed mini-floating-polypill for Parkinson's disease: combination of levodopa, benserazide, and pramipexole in various dosing for personalized therapy. Pharmaceutics 14 (5), 931.

Xu, X., Jiang, L., Zhou, Z., Wu, X.-F., Wang, Y., 2012. Preparation and properties of electrospun soy protein isolate/polyethylene oxide nanofiber membranes. ACS Appl. Mater. Interfaces. 4, 4331–4337.